Latin American Journal of Solids and Structures
www.lajss.org

A new FEM procedure for transverse and longitudinal vibration analysis of thin rectangular plates subjected to a variable velocity moving load along an arbitrary trajectory

Abstract

A combined plate element is presented for the analysis of transverse and longitudinal vibrations of a thin plate which carries a load moving along an arbitrary trajectory with variable velocity. Depending on the acceleration of the point load on its trajectory on the plate surface, the combined element, which is a combination of the 24 DOF plate element and an *equivalent mass element*, represents transverse (z) inertia, Coriolis and centripetal and longitudinal (x, y) inertia effects of the moving load. In order to obtain the combined element, mass, damping and stiffness matrices of the *equivalent mass element* representing the mass are first derived by using the relations between nodal forces, nodal deflections and deflection-shape functions of the plate element and the inertia and other forces of the moving mass according to the global coordinates on the plate and local coordinates on the plate element. Then, the obtained property matrices of the *equivalent mass element* and property matrices of the plate element were added together in order to obtain the combined plate element. For verification, the suggested technique was applied on a simply supported beam-plate under a moving load, and agreements were obtained with existing literature. In addition, intensive analysis and simulations were conducted at different dimensionless mass rates (mass of the load/mass of the plate) and angular velocities for a circular motion on a CCCC plate, and the results are provided. Furthermore, analysis results are provided for moving force condition which neglects the inertia, Coriolis and centripetal effects of the load, and it was shown that the moving mass assumption generated very different results with moving load assumption especially at high mass ratio and velocity values. Analysis results made it clear that the dynamic behaviour of the plate was differently affected by an orbiting mass depending on its mass ratio, orbiting radius and angular velocity

Keywords

Orbiting mass; combined plate element; plate vibrations; moving load.

İsmail Esen

Karabük University, Balıklar Kayası Mevkii, 78050, Karabük, Turkey

Corresponding author:
iesen@karabuk.edu.tr

http://dx.doi.org/10.1590/1679-78251525

Received 19.08.2014
In revised form 23.12.2014
Accepted 20.02.2015
Available online 10.04.2015

1 INTRODUCTION

Vibration of solids and structures under moving loads is a significant problem for civil and machine constructions and has been studied by several researchers. One of the important studies in this area, Nikkhoo et al. (2012), examined the dynamic behavior of a thin plate excited by a moving mass using the Eigen function expansion method, whereas some researchers investigated the dynamic behavior of a Mindlin plate (Gbadeyan and Oni, 1995; Faria and Oguamanam, 2004; Gbadeyan and Dada, 2006; Amiri et al., 2013). Among the important FEM studies, Wu (2007) presented a moving load element taking into consideration the effects of the load for the dynamic analysis of inclined plates under moving loads. In another study, Wu (2005) used scale beams and scaling laws for the analyses of a rectangular plate under the effect of a line load. Some researchers (Eftekhari and Jafari, 2012) presented a method which is the combination of differential Quadrature (DQ) method and integral Quadrature (IQ) method of the Ritz method for a vibration problem of the plates subjected to masses that travel with acceleration. Representing the moving mass with all effects in a new finite element formulation, Esen (2013) presented a method that can be used in the analysis of transverse vibrations of thin rectangular plates under the effect of constant-velocity-moving loads. In a similar fashion, the same topic was studied semi-analytically by Sharbati and Szyszkowski (2011), using a composite beam element. Similar to the mesh refinement method provided in Faria and Oguamanam (2004), dynamic behaviors of angled stratified composite plates were examined with FEM in Ghafoori and Asghari (2010). Nowadays the importance of dynamic behavior of structures subjected to accelerated loads is increasing, and some researchers (Lee, 1996; Wang, 2009; Mamandi et al., 2010; Esen, 2011) studied the dynamic behavior of composite and uniform beams under accelerated loads. Using the FEM, some researchers (Wu et al., 2001; Gerdemeli et al., 2011) have modelled the moving mass problem for beams. The separation phenomenon which can occur at some values of travelling velocities and system parameters during their travel can cause fundamental change in the dynamic behavior of structures (Lee, 1998). As for different engineering applications of moving mass structure problems, (Meirovitch, 1967; Yoshida and Weaver, 1971; Bathe, 1982; Reddy, 1984; Yang, 1986; Taheri, 1987; Bachmann, 1995; Kadivar and Mohebpour, 1998; Fryba, 1999; Wilson, 2002; Clough and Penzien, 2003; Szilard, 2004; Mohebpour et al., 2011; Oni and Awodola, 2011; Awodola, 2014) can be considered important and valuable references for analytical and FEM solutions and analysis of dynamic systems.

A plate excited by an orbiting mass has considerable importance in mechanical engineering, especially in the analysis of rotating machines. The researches that study the dynamic behaviors of disk file memory units in computer industry and circular saws widely used in wood products industry can be mentioned among additional applications. Both systems mentioned above can be modelled as circular plates excited by a moving mass (Cifuentes and Lalapet, 1992). The studies on dynamic behavior of the plates under the influence of masses moving on arbitrary trajectories on their surfaces, which are among some construction and mechanical engineering applications, are limited, and some simplified systems were analytically studied in the literature, i.e., Fayaz and Nikkhoo (2009); Nikkhoo and Fayaz (2012). In addition, taking into consideration the variable motion velocities of the mass, additional studies, which will examine the effects of variable velocity along with other effects, are needed. In analytical solutions, the analyzed system has to be simplified, so that the basic mathematical complexity encountered in moving load problems can be over-

come, which sometimes urges researchers to neglect the inertia effects of the mass and the damping in the system, and in some cases, moreover, it causes simplification of the geometry and prevents the acquisition of the real behavior of the designed system. Further studies are necessary to analyze the dynamic behavior of structural systems without neglecting all inertia effects and damping in the system in moving mass-structure systems and taking into consideration variable-velocity accelerating and decelerating situations of the mass as well as its motion on different trajectories on structural systems. The new method suggested by this study which does not require the limitations mentioned above has the advantage of being used by adapting to the classical finite elements method; in addition, it meets an important need by modelling the transverse and longitudinal dynamic behavior of thin plates subjected to moving loads and under variable geometry and boundary conditions, along with the damping effects of the system and convective acceleration components of the variable velocity mass as well as variable mass travel orbits.

In this paper, the discreet governing equation of motion of a thin rectangular plate on which a mass travels with variable velocity in arbitrary orbit was obtained by combining the mass, stiffness and damping matrices of the mass with the property matrices of the plate. Property matrices of the accelerated mass were calculated through the time-dependent second-order total differential of the deflection function at variable mass contact point and the nodal forces and deflections of the plate element which the moving mass applies. Inertia effects were taken into consideration in the evaluation of in-plane and out of plane dynamic responses of the plate. Using the method recommended in this study, the dynamic response of the systems under moving loads with mass motions on orbiting path which can be found in rotating machines and similar systems as well as on rectilinear path which can be found in slab type bridges and similar structural systems can be analyzed.

2 PROBLEM DEFINITION

In the formulation the following assumptions will be adopted (Fig. 1)

- The mass inertia is considered.
- The mass is always in contact with the plate.
- The plate is thin and small displacements in the plate occurred according to Kirchhoff theory.
- The plate is of constant thickness and constant mass of unit area.
- The trajectory of the mass is defined by time-dependent $x_p(t)$ and $y_p(t)$ coordinates.

Under the above assumptions and neglecting damping, the equation of motion for constant mass velocity can be written as follows:

$$D\nabla^4 w + \mu\frac{\partial^2 w}{\partial t^2} = m_p\left[g - \frac{\mathrm{d}^2 w(x_p, y_p, t)}{\mathrm{d}t^2}\right]\delta(x - x_p(t))\ \delta(y - y_p(t)) \tag{1}$$

In Eq. (1), D is the bending rigidity, $D = Eh^3/12(1-v^2)$, where E, v, and h represent Young's modulus of elasticity, Poisson's ratio and thickness respectively and μ is the mass of unit area of the plate. And $w = (w\ \ x, y, t)$ is the vertical deflection of the plate's mid-surface at point with coordinates x and y at time t, while $\delta(x - x_p(t))$ and $\delta(y - y_p(t))$ represent the Dirac-delta func-

tions in x and y directions, respectively. The symbols m_p and g are the moving mass and gravitational acceleration, respectively.

Assuming that x_p and y_p coordinates, which define the mass motion on the plate, are function of time and the acceleration $\left(\mathrm{d}^2 w(x_p,y_p,t)\big/\mathrm{d}t^2\right)$ on the right side of Eq. (1) is calculated from the second-order total differential of plate deflection function (Fryba, 1999):

$$\begin{aligned}\frac{\mathrm{d}^2 w(x_p,y_p,t)}{\mathrm{d}t^2} = [&\frac{\partial^2 w}{\partial x^2}\left(\frac{\mathrm{d}x}{\mathrm{d}t}\right)^2 + \frac{\partial^2 w}{\partial y^2}\left(\frac{\mathrm{d}y}{\mathrm{d}t}\right)^2 + \frac{\partial^2 w}{\partial t^2} + 2\frac{\partial^2 w}{\partial x \partial y}\frac{\mathrm{d}x}{\mathrm{d}t}\frac{\mathrm{d}y}{\mathrm{d}t} \\ &+ 2\frac{\partial^2 w}{\partial x \partial t}\frac{\mathrm{d}x}{\mathrm{d}t} + 2\frac{\partial^2 w}{\partial y \partial t}\frac{\mathrm{d}y}{\mathrm{d}t} + \frac{\partial w}{\partial x}\frac{\mathrm{d}^2 x}{\mathrm{d}t^2} + \frac{\partial w}{\partial y}\frac{\mathrm{d}^2 y}{\mathrm{d}t^2}]_{x=x_p(t),\ y=y_p(t)}\end{aligned} \tag{2}$$

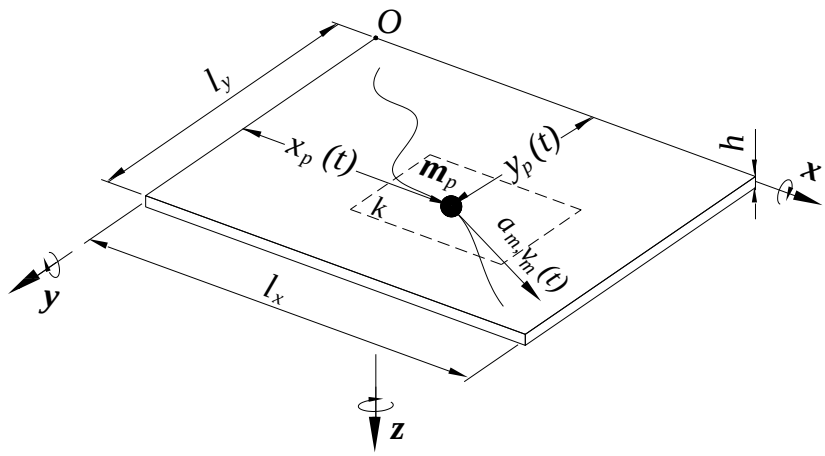

Figure 1: A moving mass travelling along an arbitrary trajectory on the surface of a rectangular plate and the kth plate element on which the moving mass applies.

The solution of the motion equation given in Eq. (1) can be obtained for any prescribed initial and boundary conditions by using analytical methods given in the literature, i.e. in Bachmann (1995); Nikkhoo and Fayaz (2012). In this study, including damping, the more accurate dynamic behaviour of the mass-plate system can be determined with the method which will be explained below. The finite element formulation of the system is obtained, evaluating the contact forces between the mass and the plate on the right hand side of the Eq. (1)

2.1 Finite element formulation of a mass that moves along an arbitrary path on a plate with variable velocity

According to the local x, y, z coordinates of the plate element seen in Figure 2 and the positions $x_m(t)$ and $y_m(t)$ of the mass on the plate element, the in-plane forces (F_x and F_y) and out-of-plane force (F_z) on p, which is the contact point induced by m_p due to the vibration and curvature of the plate element are as given in Gbadeyan and Oni (1995), respectively:

$$\begin{aligned} F_x &= m_p \ddot{\eta}_{mx}\ \delta(x - x_p(t)) \\ F_y &= m_p \ddot{\eta}_{my}\ \delta(y - y_p(t)) \\ F_z &= \left[\, m_p g - m_p \ddot{\eta}_{mz} \,\right]\delta(x - x_p(t))\delta(y - y_p(t)) \end{aligned} \tag{3.a}$$

with,

$$\ddot{\eta}_{mz} = \frac{\mathrm{d}^2 w_z(x_p, y_p, t)}{\mathrm{d}t^2},\ \ddot{\eta}_{mx} = \frac{\mathrm{d}^2 w_x(x_p, y_p, t)}{\mathrm{d}t^2} \approx a_{m_x},\ \ddot{\eta}_{my} = \frac{\mathrm{d}^2 w_y(x_p, y_p, t)}{\mathrm{d}t^2} \approx a_{m_y} \tag{3.b}$$

$$\begin{aligned} x_p &= x_0 + v_{x_0} t + \frac{a_{m_x} t^2}{2}, \quad \frac{\mathrm{d}x_p}{\mathrm{d}t} = v_{x_0} + a_{m_x} t, \quad \frac{\mathrm{d}^2 x_p}{\mathrm{d}t^2} = a_{m_x} \\ y_p &= y_0 + v_{y_0} t + \frac{a_{m_y} t^2}{2}, \quad \frac{\mathrm{d}y_p}{\mathrm{d}t} = v_{y_0} + a_{m_y} t, \quad \frac{\mathrm{d}^2 y_p}{\mathrm{d}t^2} = a_{m_y} \end{aligned} \tag{3.c}$$

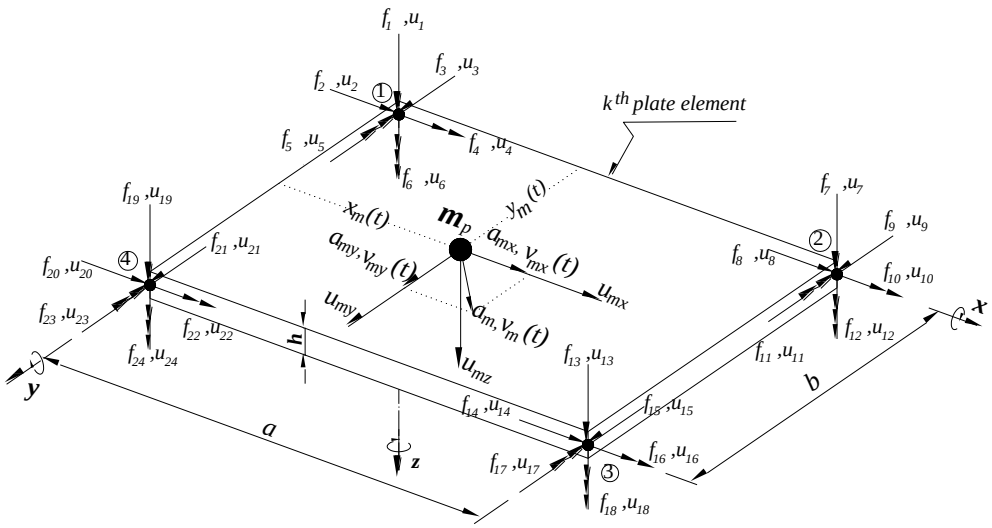

Figure 2: The rectangular plate element on which the moving mass m_p applies at time t, with dimensions a and b and equivalent nodal deflections and forces.

where $(w_x\ x_p, y_p, t), (w_y\ x_p, y_p, t), (w_z\ x_p, y_p, t)$ are deflections in x, y and z directions respectively at contact point. While x_0, y_0 and v_{x0}, v_{y0} are respectively initial positions and velocities of the mass when time is "zero"; a_{mx} and a_{my} are components of acceleration vector of the mass in x and y directions. For vibrations of the plate in longitudinal x and y directions, the derivation procedure of accelerations $\ddot{u}_{m_x}$ and $\ddot{u}_{m_y}$, in Eq. (3.b), are provided in Appendix A. For the uniformly-accelerated motion according to (3.b) and (3.c), the vertical acceleration in Eq. (2) is in the following form:

$$\begin{aligned} \ddot{\eta}_{mz} = {} & w_x''(v_{x_0} + a_{m_x} t)^2 + w_y''(v_{y_0} + a_{m_y} t)^2 + \ddot{w} + 2(v_{x_0} + a_{m_x} t)(v_{y_0} + a_{m_y} t) w_{xy}'' + 2(v_{0_x} + a_{m_x} t)\dot{w}_x' \\ & + 2(v_{y_0} + a_{m_y} t)\dot{w}_y' + a_{m_x} w_x' + a_{m_y} w_y' \end{aligned} \tag{4}$$

Eq. (4) was substituted into the last equation of (3.a). It becomes:

$$\begin{aligned} F_z = m_p \{ g - \big[& w_x''(v_{x_0} + a_{m_x} t)^2 + w_y''(v_{y_0} + a_{m_y} t)^2 + 2 w_{xy}''(v_{x_0} + a_{m_x} t)(v_{y_0} + a_{m_y} t) + a_{m_x} w_x' + a_{m_y} w_y' \\ & + \ddot{w} + 2\dot{w}_x'(v_{x_0} + a_{m_x} t) + 2\dot{w}_y'(v_{y_0} + a_{m_y} t) \big] \} \delta(x - x_p) \delta(y - y_p) \end{aligned} \tag{5.a}$$

where " $'$ ", " $\cdot$ " are, respectively, spatial and time derivatives of deflections; and, since the mass moves along the deflected shape of the plate, one can divide the vertical force F_z into three components that are

$$m_p[w''_x(v_{x0}+a_{mx}t)^2+w''_y(v_{y0}+a_{my}t)^2+2w''_{xy}(v_{x0}+a_{mx}t)(v_{y0}+a_{my}t)+a_{mx}w'_x+a_{my}w'_y] \tag{5.b}$$

$$m_p\ddot{w} \tag{5.c}$$

$$2m_p[\dot{w}'_x(v_{0x}+a_{mx}t)+\dot{w}'_y(v_{y0}+a_{my}t)] \tag{5.d}$$

Eqs. (5.b), (5.c) and (5.d) are, respectively, the centripetal force, the inertia force and the Coriolis force components. The subscripts " $_x$ " and " $_y$ " show that the function of deflection is derived by x and y, respectively.

The rectangular plate element in Figure 2 is a 24- DOF conforming plate element with $C^{(1)}$ continuity conditions at element boundaries. It includes constant twist ($\partial^2 w/\partial x\partial y$) at corner nodes. Therefore, each corner nodal deflection is (Szilard, 2004):

$$u_i=\begin{bmatrix}u_{i1} & u_{i2} & u_{i3} & u_{i4} & u_{i5} & u_{i6}\end{bmatrix}^T=\begin{bmatrix}w_z & w_x & w_y & \theta_x & \theta_y & \theta_{xy}\end{bmatrix}_i^T \tag{6}$$
$$(i=1,2,3,4:\ \text{nodes of the plate element})$$

where w_z, w_x and w_y are, respectively, the vertical deflection, the longitudinal x and y deflections of i^{th} nodal point, and θ_{x_i} and θ_{y_i}, θ_{xy_i} are, respectively, rotation about x and y-axis and twist of nodal point i.

For simplification let us use three types of indexes: i =2, 8, 14, 20 for longitudinal x, i =3, 9, 15, 21 for longitudinal y, i =1, 4, 5, 6, 7, 10, 11, 12, 13,17, 18, 19, 22, 23, 24 for transverse z and i =1, 2, ..., 24 for everything together. The following indexes can be defined as:

$$I_x=\{2,8,14,20\} \tag{7.a}$$

$$I_y=\{3,9,15,21\} \tag{7.b}$$

$$I_z=\{1,4,5,6,7,10,11,12,13,16,17,18,19,22,23,24\} \tag{7.c}$$

$$I=I_x\cup I_y\cup I_z=\{1,2,...,24\} \tag{7.d}$$

The equivalent nodal forces of the k^{th} plate element are obtained using all forces in Eqs. (3) and (5) and the shape functions of the 24 DOF plate element given in Figure 2 (Clough and Penzien, 2003; Wu, 2007):

$$f_{k_i}=\phi_i m_p\ddot{\eta}_{mx},\ (i\in I_x) \tag{8.a}$$

$$f_{k_i}=\phi_i m_p\ddot{\eta}_{my},\ (i\in I_y) \tag{8.b}$$

$$\begin{aligned}f_{k_i}=\phi_i m_p\{g-\big[&w''_x(v_{x_0}+a_{m_x}t)^2+w''_y(v_{y_0}+a_{m_y}t)^2+2w''_{xy}(v_{x_0}+a_{m_x}t)(v_{y_0}+a_{m_y}t)+a_{m_x}w'_x\\&+a_{m_y}w'_y+\ddot{w}+2\dot{w}'_x(v_{x0}+a_{m_x}t)+2\dot{w}'_y(v_{y_0}+a_{m_y}t)\big]\},\ (i\in I_z)\end{aligned} \tag{8.c}$$

where ϕ_i ($i \in I$) are shape functions of the plate element given by Szilard (2004), see Appendix. B.

The relations between shape functions and deflections (in- plane x and y deflections and out of plane z deflection) of the plate element at position x and y, and time t, are (Szilard, 2004):

$$w_x(x,y) = \sum_{i \in Ix} \phi_i u_i \tag{9.a}$$

$$w_y(x,y) = \sum_{i \in I_y} \phi_i u_i \tag{9.b}$$

$$w_z(x,y) = \sum_{i \in I_z} \phi_i u_i \tag{9.c}$$

The deflections of the contact point of the mass on the plate element in terms of the nodal deflections of the plate element can also be obtained as follows:

$$\eta_{mx} = \sum_{j \in I_x} \phi_j u_j \tag{10.a}$$

$$\eta_{my} = \sum_{j \in I_y} \phi_j u_j \tag{10.b}$$

$$\eta_{mz} = \sum_{j \in I_z} \phi_j u_j \tag{10.c}$$

where u_i ($i \in I$) are the deflections of the nodes of the plate element at which the moving mass m_p locates. Substituting Eqs. (9) and (10) into Eq. (8) and writing the resulting expressions yield:

$$f_{k_i} = \phi_i m_p \sum_{j \in I_x} (\phi_j \ddot{u}_j), (i \in I_x) \tag{11.a}$$

$$f_{k_i} = \phi_i m_p \sum_{j \in I_y} (\phi_j \ddot{u}_j), (i \in I_y) \tag{11.b}$$

$$\begin{aligned} f_{k_i} = & -\phi_i m_p g + \phi_i m_p (v_{x_0} + a_{m_x} t)^2 \sum_{j \in I_z} (\phi_j^{xx} u_j) + \phi_i m_p (v_{y_0} + a_{m_y} t)^2 \sum_{j \in I_z} (\phi_j^{yy} u_j) \\ & + 2\phi_i m_p (v_{x_0} + a_{m_x} t)(v_{y_0} + a_{m_y} t) \sum_{j \in I_z} (\phi_j^{xy} u_j) + \phi_i a_{m_x} \sum_{j \in I_z} (\phi_j^{x} u_j) + \phi_i a_{m_y} \sum_{j \in I_z} (\phi_j^{y} u_j) \\ & + \phi_i \sum_{j \in I_z} (\phi_j \ddot{u}_j) + 2\phi_i (v_{x0} + a_{m_x} t) \sum_{j \in I_z} (\phi_j^{x} \dot{u}_j) + 2\phi_i (v_{y0} + a_{m_y} t) \sum_{j \in I_z} (\phi_j^{y} \dot{u}_j), \ (i \in I_z) \end{aligned} \tag{11.c}$$

where the superscripts "x" and "y" define that the shape functions are derived by x and y, respectively. When the Eqs. (11.a), (11.b) and (11.c) are rearranged in terms of the nodal forces f, nodal deflections u, nodal velocities $\dot{u}$ and nodal accelerations $\ddot{u}$, the following matrix equation can be obtained:

$$\{f\} = [m]\{\ddot{u}\} + [c]\{\dot{u}\} + [k]\{u\} \tag{12}$$

Where,

$$\begin{aligned} \{f\} &= \begin{bmatrix} f_1 & f_2 & \dots & f_{23} & f_{24} \end{bmatrix}^T, \quad \{\ddot{u}\} = \begin{bmatrix} \ddot{u}_1 & \ddot{u}_2 & \dots & \ddot{u}_{23} & \ddot{u}_{24} \end{bmatrix}^T \\ \{\dot{u}\} &= \begin{bmatrix} \dot{u}_1 & \dot{u}_2 & \dots & \dot{u}_{23} & \dot{u}_{24} \end{bmatrix}^T, \ \{u\} = \begin{bmatrix} u_1 & u_2 & \dots & u_{23} & u_{24} \end{bmatrix}^T \end{aligned} \tag{13}$$

$$\begin{aligned} f_i &= m_p g\phi_i, \ \ (i \in I_z) \\ f_i &= m_p a_{m_x}\phi_i, \ \ (i \in I_x) \\ f_i &= m_p a_{m_y}\phi_i, \ \ (i \in I_y) \end{aligned} \tag{14}$$

In Eq. (11), all the non-zero coefficients of $[\boldsymbol{m}]_{24x24}$, $[\boldsymbol{c}]_{24x24}$ and $[\boldsymbol{k}]_{24x24}$ are

$$\begin{aligned} m_{ij} &= m_p\phi_i\phi_j, \ \ (i,j \in I) \\ c_{ij} &= 2m_p(v_{x_0} + a_{m_x}t)\phi_i\phi_j^{\,x} + 2m_p(v_{y_0} + a_{m_y}t)\phi_i\phi_j^{\,y}, \ \ (i,j \in I_z) \\ k_{ij} &= m_p(v_{x_0} + a_{m_x}t)^2\phi_i\phi_j^{\,xx} + m_p(v_{y_0} + a_{m_y}t)^2\phi_i\phi_j^{\,yy} + 2m_p(v_{x_0} + a_{m_x}t)(v_{y_0} + a_{m_y}t)\phi_i\phi_j^{\,xy} \\ &\quad + m_p a_{m_x}\phi_i\phi_j^{\,x} + m_p a_{m_y}\phi_i\phi_j^{\,y}, \ \ (i,j \in I_z) \end{aligned} \tag{15}$$

The $[\boldsymbol{m}]$, $[\boldsymbol{c}]$ and $[\boldsymbol{k}]$ matrices in the Eq. (12) obtained by addition of inertia force, Coriolis force and centripetal force which are induced by moving mass m_p, are the instantaneous mass, damping and stiffness matrices, respectively, of the *equivalent mass element* in the FEM modelling of the entire system. The position of the mass changes continuously, and so do these matrices representing the mass. The rectangular plate element given in Figure (2) has 6 deflection DOFs at nodal points at each corner; thus, the size of $[\boldsymbol{m}]$, $[\boldsymbol{c}]$ and $[\boldsymbol{k}]$ matrices that represent the travelling mass are identical to the element matrices of the plate element, which is 24x24. The following section will deal in detail with that, when simulating the dynamic behaviour of the plate due to mass motion, the instant overall mass, damping and stiffness matrices of the entire system during time integration of the equation of motion of the system are being reconstructed by combining $[\boldsymbol{m}]$, $[\boldsymbol{c}]$ and $[\boldsymbol{k}]$ matrices which change at every Δt time step.

2.2 Equation of motion of a plate under the influence of a moving mass

The equation of motion of a system consisting of a moving mass and plate is as follows:

$$[\bar{M}]\{\ddot{z}(t)\} + [\bar{C}]\{\dot{z}(t)\} + [\bar{K}]\{z(t)\} = \{\bar{F}(t)\} \tag{16}$$

where $[\bar{M}]$, $[\bar{C}]$ and $[\bar{K}]$ are mass, damping and stiffness matrices of the entire system respectively at time t, whereas $\{\ddot{z}(t)\}$, $\{\dot{z}(t)\}$ and $\{z(t)\}$ are the acceleration, velocity and deflection vectors, respectively; finally, $\{\bar{F}(t)\}$ is the external force vector of the entire system.

The coefficients of mass M_e and stiffness K_e matrices of a plate element without any mass addition can be found from Szilard (2004). According to the finite element segmentation and boundary conditions of the given plate system, the overall mass M and stiffness K matrixes of the entire system are constructed from elemental M_e and K_e matrices. When there is a moving mass on the plate, the mass and stiffness matrices of the entire system can be obtained by taking into consideration the inertia and centripetal forces induced by the moving mass; therefore, the coefficients of instantaneous overall mass and stiffness matrices of the entire system are:

$$\bar{K}_{ij} = K_{ij}, \ \bar{M}_{ij} = M_{ij} \ \ (i,j = 1-n : \text{total system DOF}) \tag{17.a}$$

except for the coefficients of the element k

$$\bar{K}_{ki\ \mathrm{kj}} = K_{ki\ \mathrm{kj}} + k_{ij}\ ,\quad \bar{M}_{ki\ \mathrm{kj}} = M_{ki\ \mathrm{kj}} + m_{ij}\ \ (i,j \in I) \tag{17.b}$$

Equations (17.a) and (17.b) show that when mass is on element k, we add $[\boldsymbol{m}]$ and $[\boldsymbol{k}]$ matrices given in equation (11) to the element mass and stiffness matrices of k^{th} plate element. In order to calculate instant values of time-dependent $[\boldsymbol{m}]$, $[\boldsymbol{k}]$ and $[\boldsymbol{c}]$ matrices, it is necessary to instantly obtain the $\xi(t) = x_m(t)/a$ and $\eta(t) = y_m(t)/b$ equations representing the position of the mass on k^{th} plate element and evaluate shape functions according to $\xi(t)$ and $\eta(t)$ values and substitute them in equations (B1 and B2). For this reason, the instant values of $x_m(t)$, $y_m(t)$ and k for a constant mass velocity on a path parallel to x are determined as follows:

$$\begin{aligned} &x_m(t) = vt - (k-1)l_x \\ &y_m(t) = e,\ \text{constant} \\ &k = \text{int}(el_x/ba + vt/l_x) + 1 \end{aligned} \tag{18}$$

where int() is the integer part of the value of the expression in the parenthesis. For a variable mass velocity:

$$\begin{aligned} &x_m(t) = x_p - (k-1)l_x \\ &y_m(t) = e,\ \text{constant} \\ &k = \text{int}\ (el_x/ba + x_p/2l_x) + 1 \\ &x_p = x_0 + v_{x_0}t + a_{m_x}t^2/2 \end{aligned} \tag{19}$$

For other mass trajectories, for example, for a circular trajectory (see Figure 4), the global $x_p(t)$ and $y_p(t)$ and local of $x_m(t)$ and $y_m(t)$ positions and element k on the plate can be determined by using the radius of the circular path, l_x and l_y dimensions of the plate, angular velocity of the mass, and a and b dimensions of the rectangular plate element:

$$\begin{aligned} &x_m(t) = x_p - \text{int}\ (x_p/a)a \\ &y_m(t) = y_p - \text{int}\ (y_p/b)b \\ &x_p = l_x/2 - r\cos\theta \\ &y_p = l_y/2 - r\sin\theta \\ &k = E_m(i,j), i = \text{int}\ (x_p/a) + 1,\ \ j = \text{int}\ (y_p/b) + 1 \\ &E_m(i,j) = \ j + (i\text{ - }1)Nx,\ (i = 1:Nx,\ j = 1:Ny) \end{aligned} \tag{20}$$

where Nx and Ny are the mesh numbers in x and y directions respectively.

For other mass trajectories except linear and circular ones, if the time-dependent function of an arbitrary path on a plate can be determined, depending on this function and the velocity of the mass, by determining global $x_p(t)$ and $y_p(t)$ and local $x_m(t)$ and $y_m(t)$ positions and element k,

and using the method explained here, moving mass problems at several different trajectories can be modelled. As alternative to Eq. (20), re-meshing the plate with quadrilateral elements (available in almost every commercial FE programme) in such a pattern that the nodes can be used to define the trajectory, can be used as given by Faria and Oguamanam (2004).

In order to take into consideration the effect of damping on the structure, damping matrix can be obtained by using the Rayleigh damping theory where damping matrix C is proportional to the combination of mass and stiffness matrices (Clough and Penzien, 2003).

$$C = a_0 \bar{M} + a_1 \bar{K} \tag{21}$$

$$a_0 = \frac{2\omega_i \omega_j (\zeta_i \omega_j - \zeta_j \omega_i)}{{\omega_j}^2 - {\omega_i}^2} \tag{22.a}$$

$$a_1 = \frac{2(\zeta_j \omega_j - \zeta_i \omega_i)}{{\omega_j}^2 - {\omega_i}^2} \tag{22.b}$$

where the terms ζ_i and ζ_j are damping ratios related to natural frequencies ω_i and ω_j.

In this case, the coefficients of the overall damping matrixes of the system under moving mass are:

$$\bar{C}_{ij} = C_{ij} \ (i, j = 1 - n : \text{total system DOF}) \tag{23}$$

except for,

$$\bar{C}_{ki\ \mathrm{kj}} = C_{ki\ \mathrm{kj}} + c_{ij} \qquad (i, j \in I) \tag{24}$$

Overall force vector of the system is formed by equating all coefficients except nodal forces of element k to zero. Thus, the instant force vector of the entire system is as follows:

$$\bar{F}(t) = \begin{bmatrix} 0 & \ldots & f_{k1} & f_{k2} & \ldots & f_{k23} & f_{k24} & \ldots & 0 \end{bmatrix}^T \tag{25}$$

with $f_{ki} = f_i \ (i \in I)$ which is given in Eq. (13).

3 NUMERICAL RESULTS

3.1 Verification of the method

To verify the present method with existing literature, the Newmark direct integration method is used along with $\beta = 0.25$ and $\gamma = 0.5$ values to obtain both the solution of equation (15) and verification example, where β and γ are parameters that define the sensitiveness and stability of the Newmark procedure. It has been reported that when β takes 0.25 value and γ 0.5, this numerical procedure is unconditionally stable (Wilson, 2002).

Let us take a simple supported isotropic beam-plate transversed by a $F = 4.4$ N. The dimensional and material specifications of the plate are identical with those chosen in Reddy (1984) i.e. $I_x = 10.36$ cm; $I_y = 0.635$ cm, $h = 0.635$ cm; $E = 206.8$ GPa, $\rho = 10686.9$ kg/m^3; $T_f = 8.149$ s, where

T_f is the fundamental period. In Table 1, dynamic amplification factors (DAF), which are defined as the ratio of the maximum dynamic deflection to the maximum static deflection, are compared with several previous numerical, analytical and experimental results available in literature. It is noted that T is the required time for moving load to travel the plate. It is seen that the results obtained by the new finite element (column 3) are very close to the analytical solution Meirovitch (1967).

V (m/s)	T_f/T	1	2
15.6	0.125	1.047	1.025
31.2	0.25	1.354	1.121
62.4	0.5	1.270	1.258
93.6	0.75	1.575	1.572
124.8	1	1.706	1.701
156	1.25	1.711	1.719
187.2	1.5	1.547	1.700
250	2	1.538	1.548

(1) Present method.
(2) Analytical solution from Meirovitch (1967).

Table 1: Dynamic amplification factors (DAF) versus velocity.

3.2 Case study: Orbiting mass

In order to examine the effect of the mass that moves in an orbit on the plate, a square thin plate with all edges meeting CCCC conditions as well as with $l_x = l_y = 1$ m dimensions and $h = 0.01$ m thickness values was chosen. Other properties of the plate are identical to the previous plate. The damping matrix $\bar{C}$ of the whole system was calculated with equations (23 and 24) by using the damping ratios of $\zeta_1 = 0.005$ and $\zeta_2 = 0.006$ (which correspond to the system's natural frequencies ω_1, ω_2). Figure 4 shows a square CCCC plate which carries a mass with an angular velocity of ω at a circular path with a radius of r. The plate was divided into plate elements that it consists of 121 elements and 144 nodes with 11x11 meshing. The Cartesian coordinate system of the plate was placed at such a location where left edge and back edge combine at $x = 0$, $y = 0$, O point and the middle point of plate thickness is $z = 0$ and downward positive. Local coordinates of the plate elements were located at the left back corner similar to the plate. Global $x_p(t)$ and $y_p(t)$ coordinates of the mass on plate were evaluated depending on the coordinate system as well as the element on which the mass is located during motion, whereas local $x_m(t)$, $y_m(t)$ coordinates are evaluated depending on the local coordinate system.

Starting position of the mass is the point where ϑ angle on the trajectory is zero; the motion of the mass is clockwise with constant angular velocities. Scalar value of the tangential velocity of the mass is constant but the direction of the velocity is constantly changing; therefore, a centripetal acceleration affects the mass towards the central point of the trajectory. At any ϑ angle, the global coordinate of the mass on the plate and its local coordinate on the element are calculated with Eq. (20). The number of the element which hosts the mass is determined by matrix mapping algorithm also given in Eq. (20). Angular vibration frequencies at the first four vibration modes of the chosen plate are $\omega_1 = 567.0254$ rad/s, $\omega_2 = \omega_3 = 1154.3784$ and $\omega_4 = 1720.3322$ rad/s. Analysis is con-

ducted separately for constant angular velocities of the mass during one tour and in a certain time period ($75\,T_1$), where T_1 is the period of the first fundamental vibration mode.

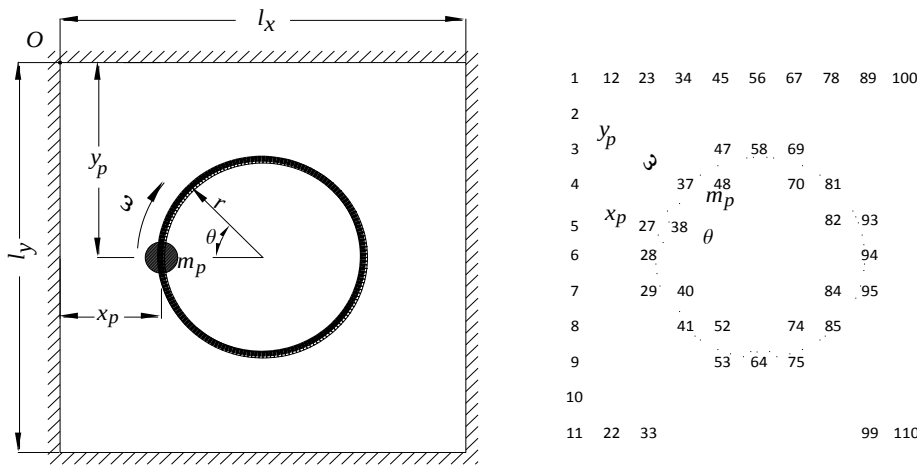

Figure 4: A CCCC plate with an orbiting mass that moves on a circular path with a radius of r and at an angular velocity of ω.

For mass ratios $\varepsilon = 0.05$, 0.1, 0.25, 0.5 and 1, the behaviour of the plate at different angular velocities and different trajectory radiuses is shown with graphics. The mass ratio ε is defined by ratio of the mass of the moving load to the mass of the plate. Figure 5 shows the dynamic deflections of the central point of the plate in one-tour motion situation of the masses with $\varepsilon = 0.05$, 0.1, 0.25 mass ratios at a circular trajectory of radius $r = 0.25$ m, which angular velocity starts at 1 up to 100 rad/s with increments of 1 rad/s. These deflections are defined as the ratio of maximum values of the absolute time-dependent deflections of the central point of the plate as DAF $= \left|\omega_{\max}(l_x/2, l_y/2, t)\right| / \omega_{st}(l_x/2, l_y/2)$ to the deflections that the mass would have generated if it had remained static at the central point of the plate. The amount of deflection that will be created by a static force at the central point of the thin plate under a square CCCC boundary conditions can be calculated with $\omega_{st}(l_x/2, l_y/2) = 0.061 m_p g l_x^{\,2} / Eh^3$ formula, Clough and Penzien (2003). The mass of the plate is 78.5 kg; moving mass is 3.925 kg, 7.85 kg 19.625 kg, 39.25 kg and 78.5 for $\varepsilon = 0.05$, 0.1, 0.25, 0.5 and 1, respectively.

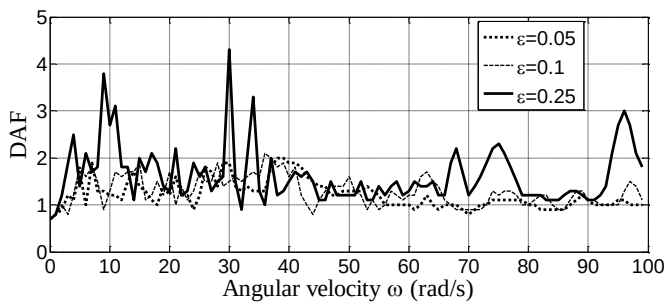

Figure 5: Angular velocity-dependent dynamic behaviour of maximum deflections that develop at the central point of the plate in case of motion with various mass ratios of the mass at circular orbit with $r = 0.25$ m, DAF (dynamic amplification factors).

Close examination of Figure 5 shows no considerable increase in deflection on the plate in masses with relatively low mass ratio, i.e. $\varepsilon = 0.05$ and 0.1. DAFs obtained in the given velocity interval are usually under 2 and fluctuate between 0.75 and 2, depending on the angular velocity of the mass. Nevertheless, when the mass ratio is $\varepsilon = 0.25$, DAF considerably increases at some angular rotation velocities. Maximum DAF is obtained as 4.3 at $\omega = 30$ rad/s velocity. The second highest DAF is witnessed as 3.82 at $\omega = 9$ rad/s velocity. The analyses here are conducted basing on one rotation of the mass, and the results show the transient effect of the mass. What kind of dynamic behaviour can be witnessed in the plate in case of a continuous effect posed by the mass at a constant angular velocity? Analyses results for this question will be provided below.

In Figure 6 the absolute deflections that are generated due to the assumption that the mass is a moving load. If the graph is examined carefully it can be seen that the graphs occur identical for all mass ratios in the case that each graph is given as DAF. It is seen that maximum DAF occurs at around 2 at $\omega = 16$, 32 and 48 rad/s angular rotation velocities at the orbit. This is no surprise as it is the result of the fact that neglects the inertia effects of the mass due to moving load assumption. These graphs once more tell that moving load approach is rather inadequate for reflecting the real behaviour of the plate. Nevertheless, at relatively smaller mass ratios, i.e. $\varepsilon = 0.05$ and 0.1 (Figure 7), it should be noted that considerable differences do not develop between moving mass and moving load assumption.

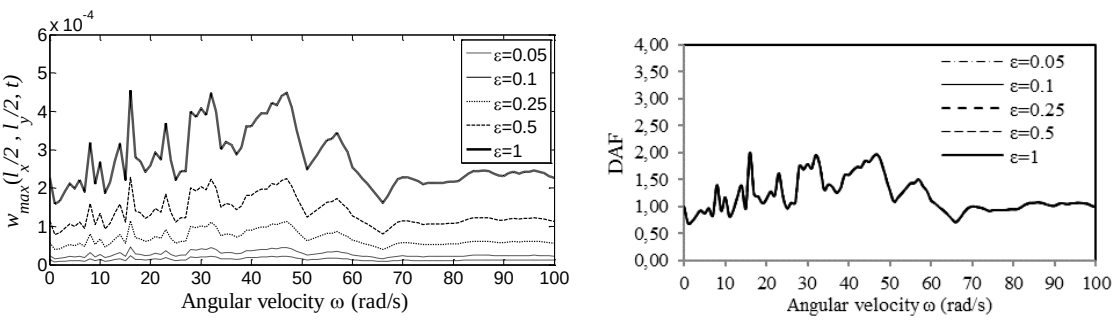

Figure 6: In the case of moving load assumption, absolute maximum deflections and DAF (dynamic amplification factors) that develop at the central point of the plate in the case of motion of the mass at various velocities and mass ratios at circular $r = 0.25$ radius.

When the mass ratio is increased, i.e. at $\varepsilon = 0.5$ value, the first resonance occurs at $\omega = 6$ rad/s and DAF increases to 10.17. The second resonance develops at $\omega = 9$ rad/s and DAF is amplified to 58.014, which is its highest value. The third peak is witnessed at $\omega = 76$ rad/s as 6.96. When the mass ratio is increased further, the peak value at $\varepsilon = 1$ develops with 778.1 at $\omega = 7$ rad/s, and it reaches 30.32 even at a very low rotation velocity such as $\omega = 3$ rad/s and changes the stability of the system. For the mass ratio $\varepsilon = 1$, the reliable angular velocity is 2 rad/s and DAF is 1.41.

The effect of the motion of the mass at different radiuses is given in Figure 8. The solid line shows the graphs for $\omega = 30$ rad/s and the dotted line shows the graphs for $\omega = 88$ rad/s. (In Figure 5, DAF reached its peak at 0.25 mass ratio and $\omega = 30$ rad/s). This velocity was particularly chosen in order to understand whether the plate behaviour remains the same or changes at this velocity and at other orbit radiuses. If the rotation velocity is $\omega = 88$, this is because the velocity

shows almost minimum DAF at all mass ratios. This velocity is chosen in order to see the plate behaviour at different radius travels.

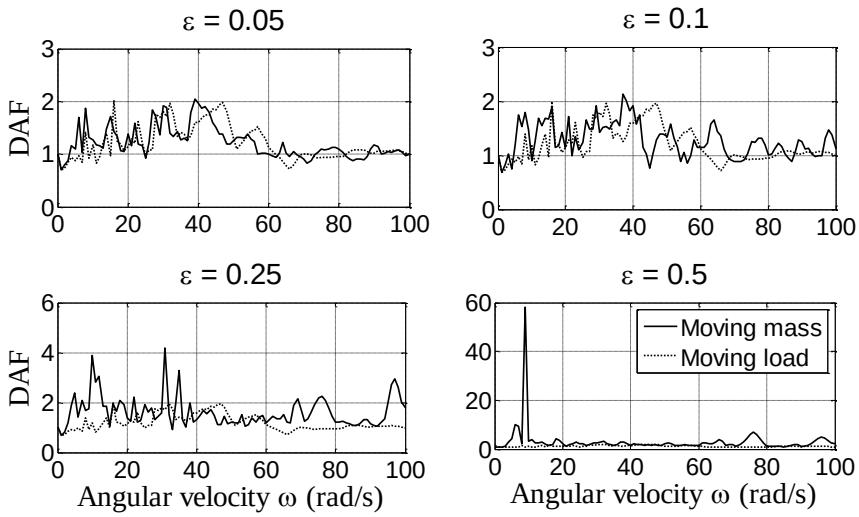

Figure 7: DAFs of absolute deflections formed on the plate by a mass moving at angular velocities $\omega = 1$-100 rad/s and $r = 0.25$ m rotation radius, depending on mass ratios; solid line is for moving mass and dotted line is for moving load.

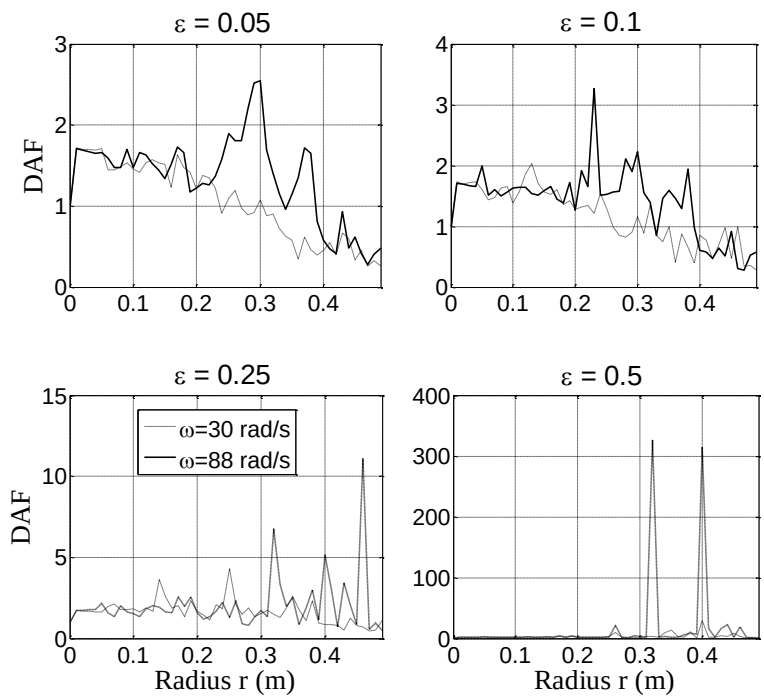

Figure 8: DAFs of central point of the plate versus rotation orbit radius r when the mass moves with $\omega = 30$ and 88 rad/s, for mass ratios of $\varepsilon = 0.05$, $\varepsilon = 0.1$, $\varepsilon = 0.25$ and $\varepsilon = 0.5$.

When Figure 8 is examined in detail, it is seen that the $\omega = 88$ rad/s rotation velocity which yields small DAF values at small mass ratios such as 0.05 and 0.1 change the stability of the system

at some radiuses at bigger mass ratios such as 0.25 and 0.5. For $\varepsilon = 0.25$ mass ratio, the radiuses of $r = 0.32$ and 0.40m and even 0.46m, which is very close to the edge of the plate, and for $\varepsilon = 0.5$ mass ratio, the radiuses of $r = 0.32$ and 0.40, are considered highly risky. At $\omega = 30$ rad/s rotation velocity, $r = 0.3$ and 0.37 m radiuses for 0.05 mass ratio, $r = 0.23$ m radius for 0.1 mass ratio, $r = 0.14$ radius for 0.25 mass ratio and $r = 0.26$, $r = 0.35$ and $r = 0.40$ m radiuses for 0.25 m and $\varepsilon = 0.5$ mass ratios are rotation radiuses where DAF reaches its peak. From these results, it can be concluded that a rotation velocity and mass ratio which is reliable for one radius will not necessarily be reliable for another radius.

Figure 9 presents the behaviour of a plate depending on mass ratios which are at a certain radius orbit, at $\omega = 30$ rad/s velocity and at a definite period of travel, i.e. $t = 75T_1$, $r = 0.375$ m, where the mass takes 4 tours a second at its orbit on the plate in $t = 0.837758$ seconds. At mass ratios of 0.05 and 0.25, deflections of the plate are small and stable, whereas at 0.1 deflections tend to increase slowly and constantly; at 0.5 and 1 mass ratios deflections tend to increase rapidly. Figure 10 gives the change generated by the effect of constant mass ratio $\varepsilon = 0.5$ at $\omega = 30$ rad/s velocity for moving mass and load assumption. As for motion at $r = 0.125$ motion orbit radius, deflections decrease in time, whereas they constantly and slowly increase at 0.25 radius; they tend to increase rapidly at 0.375 and 0.475 m and change the plate stability. Thus, it can be observed that the designs should take continuity of motion on orbit into consideration. So much so that if the plate is subjected to constant interaction with the mass at an angular velocity that corresponds to a very small peak, resonance will develop albeit slowly after some time as Figs. 9 and 10 show.

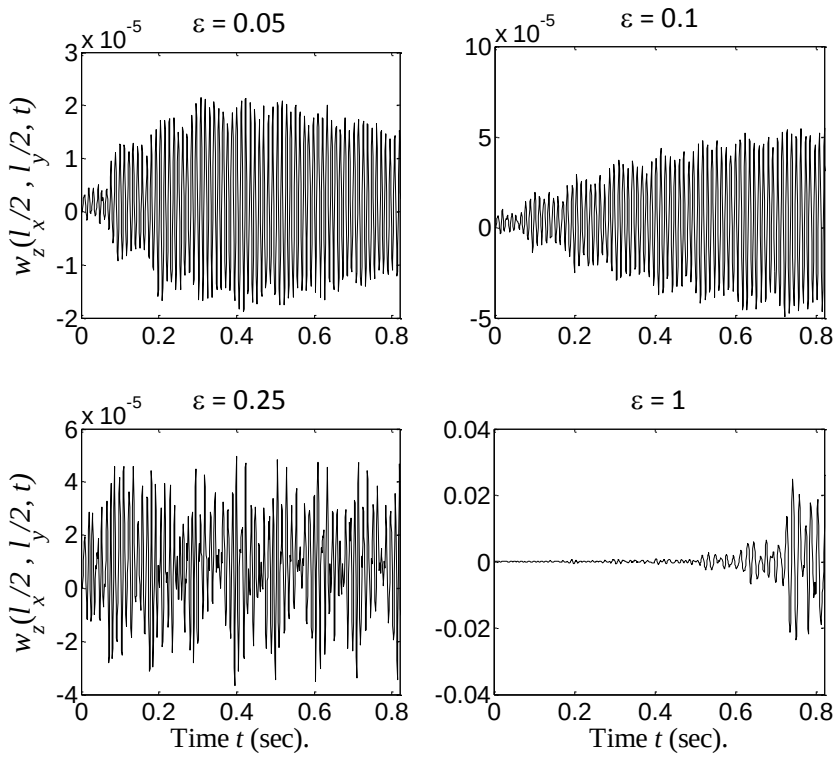

Figure 9: For an excitation period of $75T_1$, deflections of the central point of the plate for orbiting radius $r = 0.375$ m, with $\omega = 30$ rad/s and, mass ratios of $\varepsilon = 0.05$, $\varepsilon = 0.1$, $\varepsilon = 0.25$ and $\varepsilon = 1$.

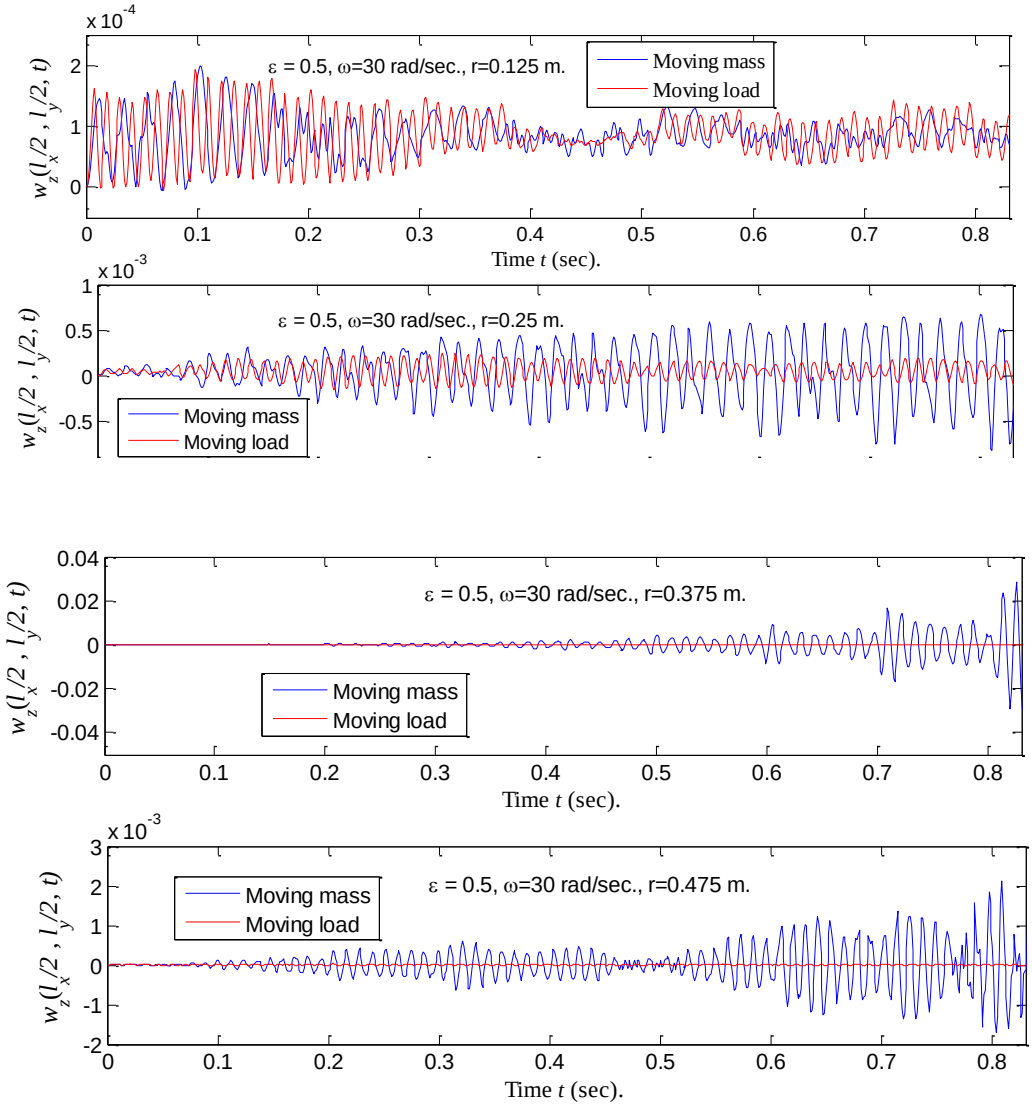

Figure 10: Deflections of the central point of the plate for: $\varepsilon = 0.5$, $\omega = 30$ rad/s., $r = 0.125, 0.25, 0.375, 0.475$ m.

Figure 11 gives the situations that examine the behaviour of the plate in the interval until the angular frequency of the first fundamental vibration mode at very high angular velocities, i.e. $\omega_1 = 576.0254$ rad/s, at an orbit with a certain radius on the plate.

In this analysis, the angular velocity was started at $\omega/\omega_1 = 0.01$, increased by 0.01 increments and reached to ω_1 velocity in 100 steps, where the 0.01 step ratio is 5.760254 rad/s, and angular velocities between two steps are not shown in the analysis. As a result, resonance developed at $\omega = 9$ rad/s velocity at $\varepsilon = 0.5$ mass ratio, but as this velocity was omitted in these graphs, this impact cannot be observed. For this reason, the graphs given below should be evaluated under the light of this reality. These graphs are provided so as to give a general idea; they also confirm that at mass motions with this kind of orbit, analysis steps should be kept as small as possible while analysing resonance behaviour of the system. As Figure 11 manifests, small mass ratios, i.e. $\varepsilon = 0.05$ and 0.1 and smaller, and at low angular rotation velocities until $0.2\omega_1$, moving mass and moving load ap-

proaches yield similar results. For this reason, at very small mass ratios and rotation velocities, moving load approach can be used for those who want to get quick results. However, as the angular velocity increases, graphs change differently. It can be seen that, for all mass ratios, graphs yield many huge or small peaks at different velocities. With more precision, analysis results for orbit radius of $r = 0.25$m with $\omega = 1$ rad/s increments, from 1 to 577 rad/s and $\varepsilon = 0.25$ mass ratio are provided in Figure 12 in 3-d fashion. For the mass ratio of $\varepsilon = 0.25$ and rotation orbit radius of $r = 0.25$ m, deflections of the central point of the plate are given in Figure 12 depending on the ϑ angle at which the mass is located on the plate and the ω angular velocity of the mass, where the vertical axis shows the real deflections of the central point of the plate, and horizontal x and y axes show the angular velocity of the mass according to the position angle of the mass as per the reference system. When Figure 12 is examined in detail, it can be seen that ϑ angles with high deflection values are mostly bigger than 180 degrees, because when the mass is rotating on the plate, the vibration velocity and acceleration of the plate system increases due to the mass motion.

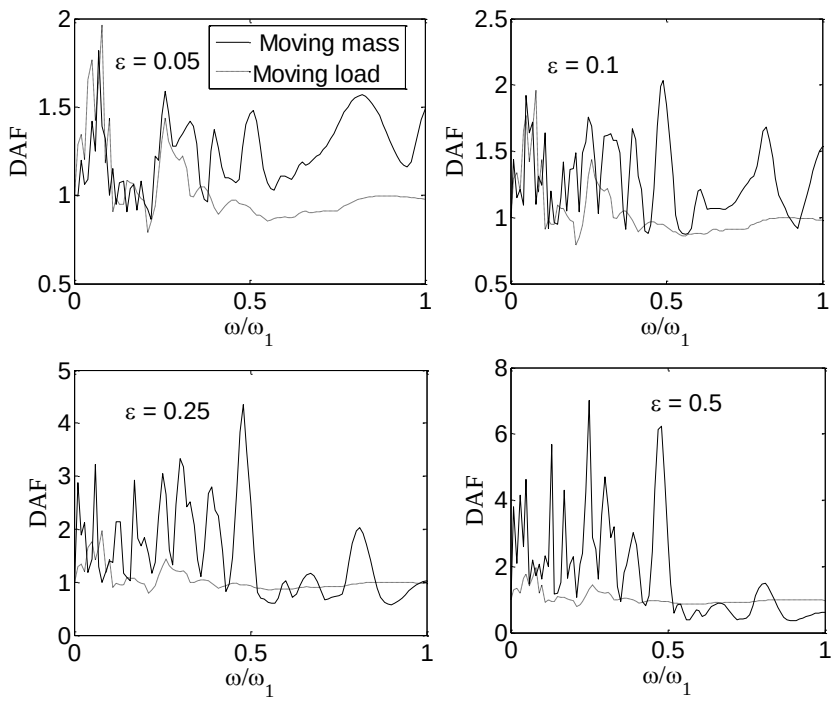

Figure 11: DAFs of central point for $\omega/\omega_1 = 0.1$-1, orbiting radius $r = 0.25$ m, $\varepsilon = 0.05$, 0.1, 0.25, 0.5, moving mass and moving load cases.

In real engineering systems, the effects of these parameters have to be controlled with very small changes in the planned working interval of the system taking into consideration the rotation velocity, mass ratio and rotation radius of the designed system. Otherwise, the system can be risked if one parameter that can create resonance in the system is gone unnoticed.

Similar situation is also witnessed in motion on a rectilinear path, Esen (2013). It is obvious that, as the mass ratio grows, the resonance affecting frequency decreases with the inverse proportion. At relatively larger mass ratios such as $\varepsilon = 0.25$ and 0.5, at angular velocity values of ap-

proximately $0.52\omega_1$ and higher, deflections that develop with the impact of high velocity and mass decrease as $[c]$ and $[k]$ matrixes repress the motion-equation of the plate. Despite all this difficulties, each mass ratio has a reliable orbiting radius and rotation velocity and each orbiting radius and rotation velocity has a mass ratio with which motion can be constantly ensured without changing the stability of the plate mass system. In practical design, the method recommended in this paper can be applied to easily determine the other reliable parameters depending on a certain parameter. For example, as can be seen in Figure 9, $r = 0.375$ m looks reliable for this plate with $\omega = 30$ rad/s, $\varepsilon = 0.05$, $\varepsilon = 0.25$ values. In Figure 10, the rotation radius of $r = 0.125$ m is reliable for $\varepsilon = 0.5$, $\omega = 30$ rad/s, whereas in Figure 8, all radiuses under $r = 0.2$ m are reliable.

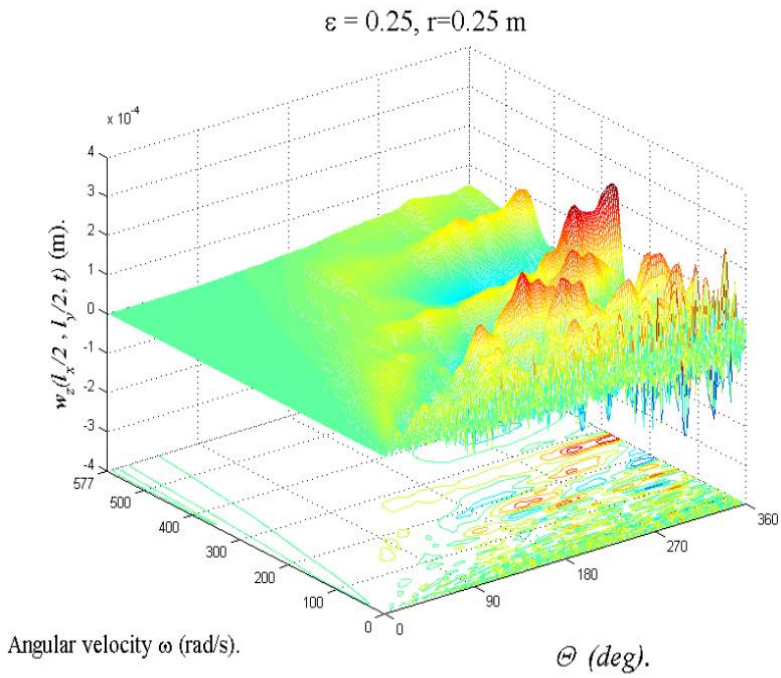

Figure 12: Deflections of the central point of the plate at $\varepsilon = 0.25$ mass ratio and $r = 0.25$ rotation orbit radius depending on the ϑ angle with which the mass is located on the plate and ω angular speed of the mass.

The longitudinal deflections of the contact point in x and y directions due to centrifugal acceleration of the moving mass are given in Figure 13, for $\varepsilon = 0.25$, $r = 0.25$ m and constant angular velocities of 10, 30 and 90 rad/s, depending on dimensionless position $(\omega t/2\pi)$ of the rotating mass around the circular path. The black lines are for direction x, while the red ones are for direction y. When the Figure 13 is examined closely, especially for higher angular velocities the longitudinal deflections of the may increase to a significant level in terms of the strength of the plate. Since the studied plate is square and isotropic, the maximum deflection for both x and y directions is 0.002972 mm; but due to rotation of the mass there is a phase angle of 90 degrees between the x and y deflections as shown from Figure 13. As another result, one can estimate that the longitudinal deflections will increase with the rise in the amount of the mass, the rotation radius and angular velocity.

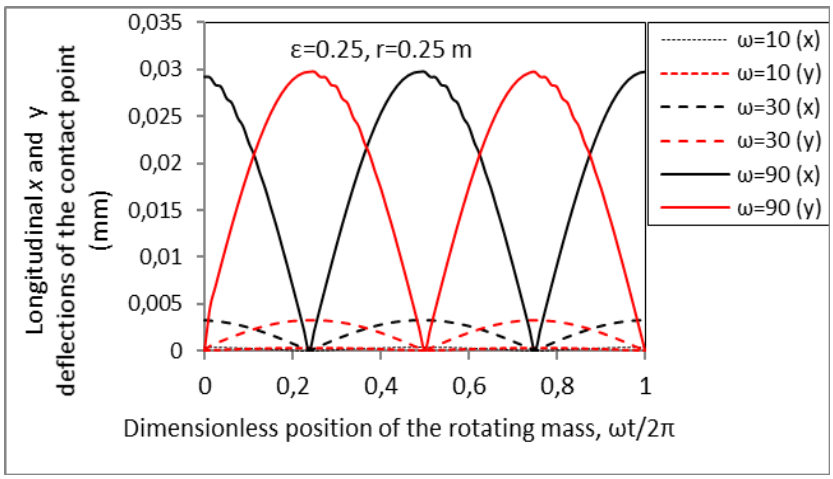

Figure 13: For angular velocities of 10, 30 and 90 rad/s, the longitudinal x and y deflections of the contact point of the plate at $\varepsilon = 0.25$ mass ratio and $r = 0.25$ m rotation orbit radius depending on the dimensionless position ($\omega t/2\pi$).

4 CONCLUSIONS

Equation of motion of a thin rectangular plate under the excitement of a moving mass has been derived representing all effects of the mass by taking into consideration the in-plane and out of plane acceleration components of the mass. In the finite element model of the equation of motion, the inertia effects induced by moving mass have been integrated to the system by deriving time-dependent equivalent mass $[m]$, damping $[c]$ and stiffness $[k]$ matrices which represent the inertia force, the Coriolis and centrifugal force components, respectively. As an alternative to the analytical methods which are disadvantaged due to the fact that it is almost impossible to reach a solution taking into consideration inertia effects, damping and variable mass velocities in plate systems under the effect of a mass that moves on variable passage paths, the author presented a method that takes into account effects discarded in the moving FORCE model. The proposed method can be used for the calculation of the dynamic behaviour of moving mass-plate system along with variable mass-travelling velocities and all effects of the mass and vibration damping effects of the system for various mass trajectories and which can be easily implemented by adapting to the classical FEM method.

For the orbiting motion, it has been indicated that, besides the size and angular velocity of the mass, the radius of the orbit is also an essential factor in behaviour of the plate. Moreover, it has been shown that larger masses rapidly decrease the resonance excitation frequency. The changes in orbiting motion of continuous rotating for time $t = 75T_1$ s have been simulated, and it has been understood that the results of a transient one-tour motion and continuous motion are rather dissimilar and that orbiting motion can generate more non-linear results. In continuous orbiting motion, the vibration velocity of the system increases, and thus the kinetic energy, system gains more energy in time which can cause resonance of the system. For this reason, this paper recommends that, in orbiting motion analyses, in order to comprehend the steady state behaviour of the system, the analyses should be based on at least four tours or a time of $75T_1$ second affecting on the plate

at selected mass size, rotation angular velocity and determined orbit radius parameters. Despite the non-linear behaviour of the system in orbiting motion, each mass ratio has a reliable orbiting radius and rotation velocity, and each orbiting radius and rotation velocity has a mass ratio with which motion can be constantly ensured without changing the stability of the plate mass system.

The most important one of the few parameters that administers the general behaviour of the plate is the change in vibration frequency of the system depending on the size and position of the mass on the plate. In orbiting motion, there are some additional factors such as the effect of velocity, deflexion of the velocity vector with the effect of centripetal acceleration, and positive or negative signs of the components of tangent velocity at some mass contact angles depending on the plate coordinate system. All these impacts non-linearly affect motion equations and the behaviour of the system. In practical design, other reliable parameters can be easily determined depending on a certain parameter applying the method recommended in this study.

Acknowledgements

The author acknowledges Sabriyaman Inc. (Manufacturer of wood working machineries in Istanbul, Turkey) for all supports to the present research.

References

Amiri, J.V., Nikkhoo, A., Davoodi, M.R., Hassanabadi, M.E., (2013). Vibration analysis of a Mindlin elastic plate under a moving mass excitation by eigenfunction expansion method. Thin Wall. Struct. 62: 53-64.

Awodola, T.O., (2014). Flexural motions under moving concentrated masses of elastically supported rectangular plates resting on variable winkler elastic foundation. Latin American Journal of Solids and Structures 11(9): 1515-1540.

Bachmann, H., (1995). Vibration Problems in Structures. Birkhauser Verlag, Berlin.

Bathe, K.J., (1982). Finite element procedure in engineering analysis. Prentice-Hall, New Jersey.

Cifuentes, A., Lalapet, S., (1992). A general method to determine the dynamic response of a plate to a moving mass. Comput. Struct. 42: 31-36.

Clough, R.W., Penzien, J., (2003). Dynamics of structures, 3rd ed. Computers and Structures, Inc., California.

Eftekhari, S.A., Jafari, A.A., (2012). Vibration of an initially stressed rectangular plate due to an accelerated travelling mass. Sci. Iran A 19(5): 1195-1213

Esen, İ., (2011). Dynamic response of a beam due to an accelerating moving mass using moving finite element approximation. Math. Comput. Appl. 16(1): 171-182.

Esen, İ., (2013). A new finite element for transverse vibration of rectangular thin plates under a moving mass. Finite Elem. Anal. Des. 66: 26-35

Faria A.R., Oguamanam, D.C.D., (2004). Finite element analysis of the dynamic response of plates under traversing loads using adaptive meshes. Thin Wall. Struct. 42: 1481-1493.

Fayaz R.R., Nikkhoo, A., (2009). Application of active piezoelectric patches in controlling the dynamic response of a thin rectangular plate under a moving mass. Int. J. Solids Struct. 46: 2429-2443.

Fryba, L., (1999). Vibrations of the Solids and Structures under Moving Loads. Thomas Telford Publishing House, London.

Gbadeyan, J.A., Dada, M.S., (2006). Dynamic response of a Mindlin elastic rectangular plate under a distributed moving mass. Int. J. Mech. Sci. 48: 323-340.

Gbadeyan, J.A., Oni S.T., (1995). Dynamic behaviour of beams and rectangular plates under moving loads. J. Sound Vib. 182 (5): 677-695.

Gerdemeli, İ., Esen, İ., Özer, D., (2011). Dynamic response of an overhead crane beam due to a moving mass using moving finite element approximation. Key. Eng. Mat. 450: 99-104.

Ghafoori, E., Asghari, M., (2010). Dynamic analysis of laminated composite plates traversed by a moving mass based on a first-order theory. Compos. Struct. 92(8): 1865-1876.

Kadivar, M.H., Mohebpour, S.R., (1998). Finite element dynamic analysis of unsymmetric composite laminated beams with shear effect and rotary inertia under the action of moving loads. Finite Elements in Analysis and Design. 29: 259.

Lee, H.P., (1996). Transverse vibration of a Timoshenko beam acted upon by an accelerating mass. Appl. Acoust. 47(4): 319-330.

Lee, U., (1998). Separation between the flexible structure and the moving mass sliding on it. J. Sound Vib. 209(5): 867-877.

Mamandi, A., Kargarnovin, M.H., Farsi, S., (2010). An investigation on effects of travelling mass with variable velocity on nonlinear dynamic response of an inclined Timoshenko beam with different boundary conditions. Int. J. Mech. Sci. 52: 1694-1708.

Meirovitch, L., (1967). Analytical methods in vibrations. The Macmillan Company. New York.

Mohebpour, S.R., Malekzadeh, P., Ahmadzadeh, A.A., (2011). Dynamic analysis of laminated composite plates subjected to a moving oscillator by FEM. Composite Structures 93: 1574–1583.

Nikkhoo, A., Fayaz R.R., (2012). Parametric study of the dynamic response of thin rectangular plates traversed by a moving mass. Acta Mech. 223: 15-27

Oni, S.T., Awodola, T.O., (2011). Dynamic behaviour under moving concentrated masses of simply supported rectangular plates resting on variable Winkler elastic foundation. Latin American Journal of Solids and Structures 8: 373-392.

Reddy, J.N., (1984). Energy and variational methods in applied mechanics. John Wiley and Sons, New York.

Shadnam, M.R., Mofid, M., Akin, J.E., (2001). On the dynamic response of rectangular plate, with moving mass. Thin Wall. Struct. 39: 797-806

Sharbati, E., Szyszkowski, W., (2011). A new FEM approach for analysis of beams with relative movements of masses. Finite Elem. Anal. Des. 47: 1047-1057

Szilard, R., (2004), Theories and Applications of Plate Analysis. Wiley, New Jersey.

Taheri, M.R., (1987). Dynamic response of plates to moving loads, structural impedance and finite element methods, Ph.D. Dissertation, Purdue University, IN.

Wang ,Y.M., (2009). The transient dynamics of a moving accelerating/decelerating mass travelling on a periodic-array non-homogeneous composite beam. Eur. J. Mech. A-Solid 28: 827-840.

Wilson, E.L., (2002). Static and Dynamic Analysis of Structures, Chapter 20: Dynamic analysis by numerical integration, Computers and Structures Inc., California.

Wu, J.J., (2005). Dynamic analysis of a rectangular plate under a moving line load using scale beams and scaling laws. Comput. Struct. 83: 1646-1658.

Wu, J.J., (2007). Vibration analyses of an inclined flat plate subjected to moving loads. J. Sound Vib. 299: 373-387.

Wu, J.J., Whittaker, A.R., Cartmell, M.P., (2001). Dynamic responses of structures to moving bodies combined finite element and analytical methods. Int. J. Mech. Sci. 43: 2555-2579.

Yang, T.Y., (1986). Finite Element Structural Analysis. Prentice-Hall, New Jersey.

Yoshida, D.M., Weaver, W., (1971). Finite element analysis of beams and plates with moving loads. Publ. Int. Assoc. Bridges Struct. Eng. 31: 79–195.

APPENDIX A. Derivation procedures of Eqs. (3.b)

Since the longitudinal deflections of the plate are very small when compared with the vertical deflections. The contact forces in x and y directions F_x and F_y are

$$F_x = m_p \frac{\mathrm{d}^2 w_x(x_p,y_p,t)}{\mathrm{d}t^2}\ \delta(x-x_p(t)),\quad F_y = m_p \frac{\mathrm{d}^2 w_y(x_p,y_p,t)}{\mathrm{d}t^2}\ \delta(y-y_p(t))$$

where $w_x(x_p,y_p,t)$ and $w_y(x_p,y_p,t)$, respectively, represent the longitudinal x and y displacements at positions x_p, y_p and time t. In this case for the longitudinal x vibration of the plate one can obtain the following equations:

$$\frac{\mathrm{d}w_x(x_p,y_p,t)}{\mathrm{d}t} = \frac{\partial w_x(x,t)}{\partial x}\frac{\partial x}{\partial t} + \frac{\partial w_x(x,t)}{\partial t}\frac{\partial t}{\partial t} + 0 + 0 = w_x'(x,t)\dot{x} + \dot{w}_x(x,t) \approx \dot{w}_x(x,t) \tag{A1}$$

$$\frac{\mathrm{d}^2 w_x(x_p,y_p,t)}{\mathrm{d}t^2} = \frac{\partial \dot{w}_x(x,t)}{\partial x}\frac{\partial x}{\partial t} + \frac{\partial \dot{w}_x(x,t)}{\partial t}\frac{\partial t}{\partial t} + 0 + 0 = \dot{w}_x'(x,t)\dot{x} + \ddot{w}_x(x,t) \approx \ddot{w}_x(x,t) \tag{A2}$$

For the longitudinal y vibration of the plate one can:

$$\frac{\mathrm{d}w_y(x_p,y_p,t)}{\mathrm{d}t} = 0 + 0 + \frac{\partial w_y(y,t)}{\partial y}\frac{\partial y}{\partial t} + \frac{\partial w_y(y,t)}{\partial t}\frac{\partial t}{\partial t} = w_y'(y,t)\dot{y} + \dot{w}_y(y,t) \approx \dot{w}_y(y,t) \tag{A3}$$

$$\frac{\mathrm{d}^2 w_y(x_p,y_p,t)}{\mathrm{d}t^2} = 0 + 0 + \frac{\partial \dot{w}_y(y,t)}{\partial x}\frac{\partial x}{\partial t} + \frac{\partial \dot{w}_y(y,t)}{\partial t}\frac{\partial t}{\partial t} = \dot{w}_y'(y,t)\dot{y} + \ddot{w}_y(y,t) \approx \ddot{w}_y(y,t) \tag{A4}$$

APPENDIX B. Shape functions of the plate element in Eq. (7).

$$\begin{aligned}
&\phi_1 = p_1q_1,\ \phi_2 = \phi_3 = (1-\xi(t))(1-\eta(t)),\ \phi_4 = p_2q_1,\ \phi_5 = p_1q_2,\\
&\phi_6 = p_2q_2,\ \phi_7 = p_1q_3,\ \phi_8 = \phi_9 = \xi(t)(1-\eta(t)), \phi_{10} = p_2q_3,\\
&\phi_{11} = p_1q_4,\ \phi_{12} = p_2q_4,\ \phi_{13} = p_3q_3,\ \phi_{14}{=}\phi_{15} = \xi(t)\eta(t),\\
&\phi_{16} = p_4q_3,\ \phi_{17} = p_3q_4,\ \phi_{18} = p_4q_4,\ \phi_{19} = p_3q_1,\\
&\phi_{20}{=}\phi_{21}{=}\eta(t)(1-\xi(t)),\ \phi_{22} = p_4q_1,\ \phi_{23} = p_3q_2,\ \phi_{24} = p_4q_2
\end{aligned} \tag{B1}$$

With,

$$\begin{aligned}
&p_1 = 1-3\xi(t)^2+2\xi(t)^3,\ p_2 = a[\xi(t)-2\xi(t)^2+\xi(t)^3],\\
&p_3 = 3\xi(t)^2-2\xi(t)^3, \qquad p_4 = a[\xi(t)^3-\xi(t)^2]\\
&q_1 = 1-3\eta(t)^2+2\eta(t)^3,\ q_2 = b[\eta(t)-2\eta(t)^2+\eta(t)^3]\\
&q_3 = 3\eta(t)^2-2\eta(t)^3, \qquad q_4 = b[\xi(t)^3-\xi(t)^2]\\
&\xi(t) = \frac{x_m(t)}{a}, \qquad \eta(t) = \frac{y_m(t)}{b}
\end{aligned} \tag{B2}$$

where p_n and q_n ($n=1, 2, 3, 4$) are hermitical polynomial components that represent plate shape functions in x and y-axes respectively. The symbols a and b are the length and width of k^{th} plate element respectively, whereas $x_m(t)$ and $y_m(t)$ are variable distances between the moving mass and the left end-local coordinate of the k^{th} plate element, at time t, as shown in Figure (2).